

# Visualizing Small Intra-cranial Arteries using TOF with Compressed Sensing

J. Yerly<sup>1,2</sup>, M. L. Lauzon<sup>2,3</sup>, and R. Frayne<sup>2,3</sup>

<sup>1</sup>Department of Electrical and Computer Engineering, University of Calgary, Calgary, AB, Canada, <sup>2</sup>Foothills Medical Centre, Seaman Family MR Research Centre, Calgary, AB, Canada, <sup>3</sup>Departments of Radiology, and Clinical Neurosciences, University of Calgary, Calgary, AB, Canada

**Introduction:** Time-of-flight (TOF) magnetic resonance angiography<sup>1</sup> (MRA) has been successfully used to diagnose vascular pathologies, such as stenoses, and aneurysms. However, the visualization of stenosis has mainly been limited to large arteries, such as the iliac, renal, and carotid arteries, as well as the middle and proximal cerebral arteries. Imaging stenoses in smaller arteries, such as smaller intracranial vessels, requires acquiring high-resolution images. This task is particularly challenging in three-dimensional (3D) TOF data acquisition because of the critical tradeoff between spatial resolution, acquisition time and signal-to-noise ratio (SNR). That is, higher spatial resolution is achieved at the detriment of longer acquisition time and lower SNR. Several approaches exist for accelerating MR imaging, such as parallel imaging<sup>2</sup> and compressed sensing<sup>3</sup> (CS). These approaches may prove favorable for accurate reconstruction of undersampled  $k$ -space datasets, thus potentially allowing the reduction of acquisition time. In addition, CS has beneficial denoising properties<sup>2</sup>, which can help improve the SNR. Here, we investigated the potential of improving the spatial resolution by using the CS paradigm to acquire and reconstruct vastly under-sampled high-resolution TOF  $k$ -space datasets, while maintaining reasonable scan time and SNR.

**Method:** On a 3-T MR scanner (Signa VH/i; General Electric Healthcare, Waukesha, WI, USA), we modified a 3D clinical TOF vascular sequence in order to acquire an undersampled set of  $k$ -space phase encodes in the  $k_y$ - $k_z$  plane. To satisfy the CS requirement of incoherent aliasing interferences from the undersampling, the phase encode locations were randomly selected based on a probability density function (PDF). This scheme ensured selection of more samples near the centre compared to the periphery of  $k$ -space. Using an 8 channel head array coil, we acquired a sparse dataset by  $10\times$  undersampling the  $k$ -space with the following parameters: repetition time (TR) = 30 ms, echo time (TE) = 3.5 ms, flip angle  $30^\circ$ , acquisition matrix size =  $160 \times 750 \times 400$ ,  $FOV_x \times FOV_y \times FOV_z = 8 \text{ cm} \times 15 \text{ cm} \times 8 \text{ cm}$ , and image resolution =  $500 \mu\text{m} \times 200 \mu\text{m} \times 200 \mu\text{m}$ . We reconstructed each  $k_y$ - $k_z$  slice in the 3D volume via CS and zero filling (ZF) reconstructions. For the CS reconstruction, we used both the wavelet and image domains as sparse domains and adjusted the regularization parameters accordingly through visual inspection of the reconstructed images. The stacks of reconstructed images were then qualitatively assessed visually by comparing individual reconstructed images and maximum intensity projection<sup>4</sup> (MIP) of the whole data volumes.

**Results:** The side-by-side 2D image comparison of the CS and ZF reconstructions showed that, with adequate and judicious selection of the regularization parameters, the CS approach resulted in sharper and less noisy images when compared to the ZF approach (Figs 1a-b vs 1c-d). The CS approach filtered out most of the aliasing interference, and the reconstructed images had higher SNR than the ZF approach. Figure 2a-c and 2d-f show the MIP rendered images from the coronal view of the volume for the ZF and CS approach. In the MIP images, the CS approach provided only slightly better conspicuity of the low contrast vessels when compared to the ZF approach (Figs 2b vs 2e).

**Discussions:** Although the CS approach clearly outperformed the ZF approach based on the side-by-side 2D image comparison of the source images (Fig 1), inspection of the MIP images found less of an improvement (Fig 2). This finding was not completely unexpected as the MIP algorithm searches for the maximum intensity along parallel rays cast through the volume. Therefore, the MIP procedure has an intrinsic, non-linear filtering property, which cancels out some of the noise reducing benefit of CS. In conclusion, variable density sampling and CS reconstruction can produce TOF images with moderate-to-high accuracy from significantly fewer  $k$ -space samples than suggested by the Nyquist-Shannon sampling theorem. This property makes it possible to notably reduce acquisition time, and allows for high-resolution TOF images, which could potentially be used to diagnose stenoses in smaller arteries, such as lenticulostriate arteries associated with lacunar stroke (see Fig. 2c and 2f).

1. Dumoulin CL, *et al.* Magn Reson Med 1989; 11: 35.
2. Lustig M, *et al.* Magn Reson Med 2007; 58: 1182.

3. Blaimer M, *et al.* Top Magn Reson Imaging 2004; 15: 223.
4. Wallis JW, *et al.* IEEE Trans Med Imaging 1989; 8: 297.

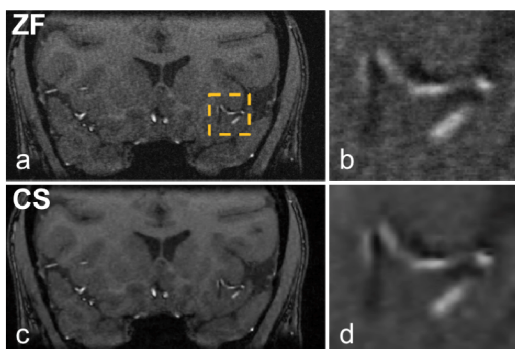


Figure 1: Side-by-side 2D image comparison of the ZF (a-b) and CS (c-d) reconstruction approaches.

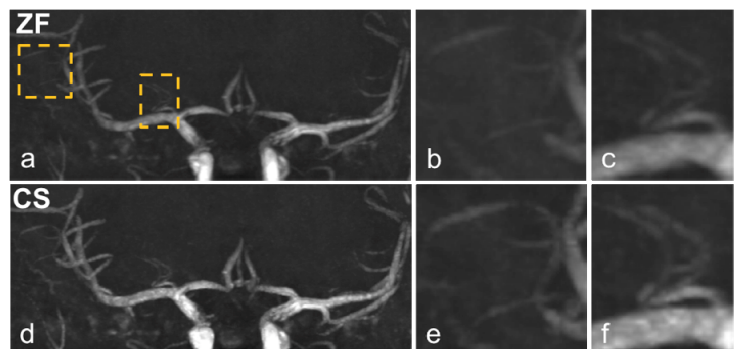


Figure 2: Comparison of the ZF (a-c) and CS (d-f) MIP rendering images from the coronal view of the reconstructed volume.